AD-A151 579 ERROR ANALYSIS OF WIND DETERMINED USING A VLF (VERY LOW FREQUENCY) OMEGA SONDE(U) WEAPONS SYSTEMS RESEARCH LAB ADELAIDE (AUSTRALIA) K H LLOYD JUN 84 WSRL-0361-TM 1/1

UNCLASSIFIED F/G 4/1 NL

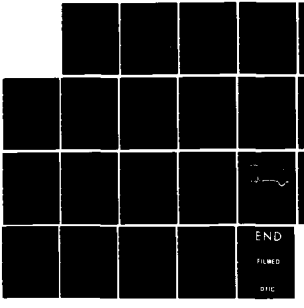

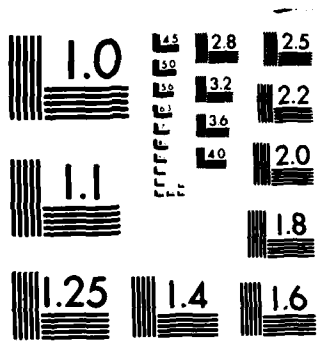

WSRL-0361-TM

AR-003-790

DEPARTMENT OF DEFENCE

DEFENCE SCIENCE AND TECHNOLOGY ORGANISATION

WEAPONS SYSTEMS RESEARCH LABORATORY

DEFENCE RESEARCH CENTRE SALISBURY
SOUTH AUSTRALIA

TECHNICAL MEMORANDUM

WSRL-0361-TM

ERROR ANALYSIS OF WIND DETERMINED USING A VLF OMEGA SONDE

K.H. LLOYD

Technical Memoranda are of a tentative nature, representing the views of the author(s), and do not necessarily carry the authority of the Laboratory.

Approved for Public Release

JUNE 1984

UNCLASSIFIED

AR-003-790

DEPARTMENT OF DEFENCE

DEFENCE SCIENCE AND TECHNOLOGY ORGANISATION

WEAPONS SYSTEMS RESEARCH LABORATORY

TECHNICAL MEMORANDUM

WSRL-0361-TM

ERROR ANALYSIS OF WIND DETERMINED USING A VLF OMEGA SONDE

K.H. Lloyd

S U M M A R Y

The atmospheric wind profile can be determined by tracking the drift of an ascending or descending sonde. Generally the sonde is tracked by radar, but, because of problems associated with radar, Omega navigation is now sometimes used as an alternative. This Memorandum discusses the errors associated with determining the wind profile by using Omega, in particular how the error is related to the rate of descent of the sonde. This study was conducted as part of the AMPARS (Artillery Meteorological Parameters Acquisition Rocket System) feasibility study.

POSTAL ADDRESS: Director, Weapons Systems Research Laboratory,
Box 2151, GPO, Adelaide, South Australia, 5001.

UNCLASSIFIED

TABLE OF CONTENTS

LIST OF TABLES

LIST OF FIGURES

1. INTRODUCTION

A perennial problem for the Army Artillery Meteorological Section is to provide rapid, accurate profiles of the atmospheric wind, temperature and humidity, which are measured in that part of the atmosphere through which the shell passes. Although the standard balloon borne radio sonde provides accurate data, it takes an hour to complete an ascent, and the balloon may drift in a direction opposite to that for which data is required.

For these reasons Army Research Requests, 80/142 and 81/110, have been raised on DSTO to investigate a rocket launched meteorological system, called the Artillery Meteorological Parameters Acquisition Rocket System (AMPARS). In this proposed system a sonde containing temperature, pressure and humidity sensors descends by parachute, having been ejected from the rocket nose at apogee. Wind is determined by drift of the sonde. This could be done, as is currently done for the balloon borne sonde, by radar. However, a radar is a bulky piece of equipment with its own peculiar problems, and it has been suggested that the path of the sonde, and hence the wind profile, could be determined using standard VLF navigation techniques. This paper investigates this proposal. There are two major VLF systems in operation, Omega and Loran; we shall confine our attention to the former, as it covers all of Australia and its surrounding oceans.

In the next section we give a very brief outline of the Omega system, drawing attention to references from which further details may be obtained. In Section 3 we discuss VLF atmospheric noise. This is produced by lightning, and sets the fundamental limit on the accuracy of determination of the phase of the received Omega signal. Section 4 discusses and gives references to, the practical cases, mainly in the USA, where Omega has been used in balloon borne and parachute carried meteorological sondes. These have all been used for gathering data for large scale atmospheric - oceanographic measuring projects.

Section 5 discusses the important subject of data analysis. Our main purpose will be to examine propagation of error variance in the data analysis. We are particularly concerned at determining which parameters are critical to the accuracy with which wind can be determined, and what be the functional dependence. It will be shown that wind error depends on signal-to-noise ratio (obtained from Sections 2 and 3), the data analysis algorithms, the positions of transmitters and receiver and the averaging time of the data. An efficient data processing algorithm is essential for reducing the time over which a signal has to be integrated to obtain accurate wind data. We wish to have as short time as is compatible with the required accuracy, because otherwise too tight a constraint is imposed on the descent rate of the sonde.

Section 6 compares the estimates of errors made in Section 5 with reported errors of measurements using Omega sondes.

2. ELEMENTS OF VLF OMEGA NAVIGATION

2.1 VLF propagation

Very low frequency radio waves (VLF) have the property of being transmitted over long distances with very little attentuation and highly stable phase characteristics. Although there is a diurnal phase variation, due to changes in the reflecting layer of the ionosphere from day to night, it is fairly reproducible from day-to-day and can be calibrated out. Examples of day-to-day variation in phase are shown in figure 1, which is taken from Beukers(ref.1). It is seen that although the diurnal variation is about 60 cec (1 centicycle = 0.01 cycle and corresponds to a position error of

300 m at 10 kHz), the day-to-day variability is about 10 cec, being generally worse at night-time. For our application, in which we are not interested in the absolute position but differences in position (ie velocity) it is the unpredicted rate of change in phase which concerns us. An error in phase rate of 1 centicycle/min is equivalent to a velocity error of 5 ms^{-1}; note that this is a bias error.

At distances greater than about 1000 km from the source, the electrostatic and induction fields have decayed substantially, and the radiation field can be accurately described by a combination of modes; see Watt(ref.2), Galejs(ref.3), Budden(ref.4) and Burgess and Jones(ref.5). The principle contributer to VLF propagation is the TM1 mode, although, particularly at night, there are contributions from other modes. This mixing of modes causes errors in the navigation using VLF. Extensive calculations on the propagation of VLF waves, including the effects of latitude and azimuth, have been made using the derived theoretical expressions; results are given, for example, by Morris(ref.6).

2.2 Omega nagivation

Omega is a world-wide navigation system based on eight VLF transmitters at large spacings; see Kaspar(ref.7), Thompson(ref.8), Hogle(ref.9), for an overview of Omega navigation system concepts. Each transmitter goes through a 10 s cycle transmitting each of the three standard omega frequencies: 10.2, 11.05 and 13.6 kHz; figure 2 shows the Omega signal transmission format. Figure 3 gives an example of Omega signal strength as a function of distance from the transmitter, Lynn(ref.10). The oscillations in amplitude and phase at night, worse nearer the transmitter, are due to the mode mixing referred to above.

There are several methods of using these signals for the determination of the position of the receiver, ie for navigation. The one most commonly used for velocity determination is the hyperbolic method illustrated in figure 4. The coherent radiation field from the tranmitters T_1 and T_2 have the circular lines of constant phase as shown. The lines of constant phase difference are the hyperbolae, also shown. Therefore a receiver, with the necessary phase stability, will be able by measuring the difference in phase of signals received from T_1 and T_2 to plot a series of hyperbolae, known as lines of position, on which its position must lie. The decision as to which hyperbola the receiver lies, called lane resolution, is made by knowing the approximate position of the receiver. The intersection of this hyperbola with another generated by a second pair of transmitters, T_3, T_4, gives a fix of position. Maximum accuracy is gained if these two hyperbolae cross at right angles; the increase in error which results from non-normal intersection is given by a factor called geometric dilution of precision (GDOP).

Although measurement errors are discussed in detail later, it is appropriate to mention now the terms which contribute to error:

- errors in transmitters and receiver timing. These must be accurate which is certainly the case with the transmitters, and demonstrates the need for a stable receiver.

- errors in signal propagation. The diurnal phase shift has already been discussed. There are also large phase changes caused by the ionospheric disturbances known as SID (sudden ionospheric disturbance) and PCA (polar cap absorption). These are both caused

by solar flares, and play havoc with the phases of the VLF transmissions. Unfortunately, nothing can be done to correct for these errors, other than to weed out the corresponding data.

- errors in determining phase of received signal. This depends on the VLF noise intensity due to lightning discharges and is discussed in Section 5.2. This error is reduced by lengthening the sampling time, as will be discussed in Section 5.3.

3. VLF NOISE DUE TO LIGHTNING STRIKES

There is a small amount of man-made VLF noise, mainly harmonics of the AC power systems, but by far the largest contribution to VLF noise comes from lightning. We shall discuss this noise in sufficient depth to be able to use the results in the next section. Further discussion is given in Watt(ref.2) and Galejs(ref.3).

Each lightning discharge is a complicated process which involves leaders and a return stroke. The bulk of the radiated power comes from the return stroke, and the spectrum of the power from an individual stroke has broad maximum in the frequency range 5 to 20 kHz. The median level of spectrum of the atmospheric noise level at 10 kHz in the Australian region lies in the range 20 to 200 μV/m per root Hertz. Table 1 gives values of expected VLF atmospheric noise around Australia; the data are CCIR data taken from Watt(ref.2). Care must be taken in using these data in estimating signal-to-noise ratio, because the noise is impulsive and has a skew distribution. This means that a receiver which has an efficient limiter or clipper will give a substantially smaller effective signal-to-noise ratio than would be expected from using the CCIR data.

Galejs(ref.2) gives observed values of the amplitude probability distribution of VLF atmospheric noise. Using these data we have calculated the reduction in mean VLF noise as a function of the limiting voltage; the results are given in Table 2. It shows, for example, that if the input signal is clipped to the level of the RMS incoming signal the RMS noise is reduced by a factor of three. This compares with the rule of thumb 15 dB (= factor of 5.6) improvement suggested by Swanson(ref.11) when a limiting receiver is used to remove the impulsive character of the log-normal noise to make it look Gaussian.

As we shall see later, receiver input bandwidth plays an important part in the error analysis. We will merely note here that, world wide, there are on average 100 lightning strikes/s, the duration of whose flash is of the order of 1 ms. Since the mean interval between strikes is 10 ms, the effects of these will be non-overlapping if we have an integrating time of the order of 2 ms or less, that is, a bandwidth of greater than 500 Hz. On the other hand, increasing the receiver bandwidth increases the noise input.

4. SURVEY OF METEOROLOGICAL SONDES USING OMEGA

This section gives a brief description of meteorological sonde systems which have been developed to use Omega for determining wind. It is intended as an introduction to the next section which examines the methods of analysis of Omega sonde data, in particular how they relate to the propagation of wind error variance.

Figure 5 shows a typical use of the Omega sonde. The Omega signals received by the sonde from the Omega transmitters are retransmitted to the ground station by telemetry. Typically 400 MHz is used as the carrier, which will

also carry the other meteorological data, such as temperature, humidity and pressure. The base station does all the data analysis; in particular, it will have the high stability oscillator necessary to determine the phase of the Omega signals.

4.1 Vaisala Microcora system

To our knowledge there is only one commercially available meteorological sonde which makes use of the Omega network to determine the atmospheric wind profile. This is manufactured by Vaisala of Finland. Unfortunately the only information we have on it is the manufacturer's glossy brochure(ref.12,13). The Met Bureau in Melbourne have bought some of these sondes for testing, together with the necessary ground equipment, but unfortunately have no knowledge of how the system functiors, in particular the constraints of VLF noise on system accuracy. As with all systems to be described, the receiver uses a vertical E field wire antenna, in this case about 1 m long, which hangs below the sonde. The Omega signals are retransmitted to ground using a 403 MHz carrier, which also multiplexes the other met data. As with the other systems to be described later, the complex data analysis which is required to get position and wind from the Omega phase data is done by a dedicated microcomputer on the ground at the base receiving station. The sonde ascends hanging below a standard meteorological balloon; as will be seen later, this slow ascent makes the task of measuring the wind profile to 1 ms^{-1} accuracy relatively easy.

The other Omega wind finding sondes on which we have unearthed information are all American, and were developed for specific large scale meteorological experiments. We will now give a brief description of each, further details are given in the valuable review paper by Govind(ref.14).

4.2 NCAR carrier balloon/Omega sonde system

This system comprises a constant altitude pressure (~30 mb, ie ~25 km) carrier balloon which releases Omega sondes. These descend on a parachute, measuring the atmospheric temperature and Omega phases as they fall. The measured raw data are telemetred to the carrier balloon where the Omega phases are related to a local reference and retransmitted to a central ground data processor via a satellite link.

The carrier balloon system (CBS) was designed for the Global Atmosphric Measurement Program, specifically for the 1977 equatorial ocean experiment, FGGE. Details of the proposed system, together with preliminary results have been given by Passi and Olson(ref.15) and Olson(ref.16). The Omega sonde receiver uses an active filter with 400 Hz bandwidth tuned to the 13.6 kHz Omega signal. Other than the preliminary trials, no results of this system appear to have been published.

4.3 NCAR dropwind sonde system

This system was developed to determine the meteorological profile in conjunction with observations by weather reconnaissance aircraft. As with the NCAR Omega sonde, this system descends by parachute after being released by the high flying (~10 km) aircraft. The received Omega signals together with the meteorological measurements are telemetered from the sonde to the aircraft, where they are processed on board the aircraft. This system was used in the GATE program. An excellent summary of the system is given by Govind(ref.17), it contains the only description of an Omega sonde which we have come across in the literature. The sonde receiver has a 150 Hz bandwidth centered on the 13.6 kHz Omega signal.

4.4 the LO-CATE system

LO-CATE (Loran/Omega - course and track equipment) is a very general position-determining system using VLF navigation, developed by the Beukers Laboratories Inc. One assumes that it would be commercially available, although the only reference we have come across it in the literature is with respect to what appears to be contractoral relations with US Government Agencies.

A general discussion of the LO-CATE system, with a brief description of the electronics of the Omega retransmitter (which could be a sonde, a bouy or any other platform whose position is to be determined) and of the base station is given by Poppe of the Beukers Laboratory(ref.18) and by Afanasjevs et al(ref.19). The application of the Beukers dropsonde and the Lo-cate system to the determination of winds below aircraft, on a contract to the US Air Force, has been described by Morrissey and Weiss(ref.20). A further application of Beukers sondes has been by NOAA in supporting the release of ship released radio sondes carrying Omega detectors (Reeves et al, reference 21). Unlike the NCAR sonde, the Beukers dropsonde retransmits the entire Omega band, 10 to 14 kHz. This enables wind to be determined using each of the three Omega transmission frequencies, thereby increasing accuracy.

4.5 Develco Ind system

Although this Omega-based position locating system is intended for application in mini remotely piloted vehicles (mini RPV) we mention it because it could be adapted for use in windsondes. Develco Inc manufactures commercially this Omega based system, which enables a mini RPV to go to waypoints which can be preprogrammed into a microprocessor which forms part of the system. Reference 22 is an information brochure put out by Develco, a description of some RPV flight trials using the full system is given by Fraser(ref.23).

5. DATA ANALYSIS AND ERROR PROPAGATION

In this section we will outline the manner in which the data is analysed, with the express purpose of determining the sources of error. As explained earlier, our main interest is to find how the accuracy of wind determination depends on the variables such as signal-to-noise ratio, bandwidth and smoothing interval of the data, but in doing so we must take cognisance of all the error sources. The data analysis, and associated sources of error can be divided into the following steps:

- propagation of the VLF signal from the Omega transmitter to the sonde,
- comparison of the phase of the received Omega signal with the local oscillator,
- determination of the rate of change of phase,
- computation of velocity from the phase rate,

We now discuss each in turn.

5.1 Ionospheric propagation

We have already discussed VLF propagation and VLF noise in Sections 2 and 3. As is shown in figure 1, the diurnal movement of the ionosphere produces phase changes at the receiver, which masquerade as position and

velocity changes. Although much of the diurnal variation can be eliminated, there remain residual day-to-day and random variation which can lead to error. We assume that changes of position are related to change of phase by $\Delta r = f\Delta\phi/Z$. The factor f is called the geometric dilution of precision, and accounts for non-optimum position of the transmitters and receivers. Taking f = 4, as fairly typical, we see that a position accuracy of 1 ms^{-1} requires the phase to change at less than 0.01°/s or, equivalently at 0.05 cec/s (one centicycle (cec) is equivalent to 3.6° and corresponds to about 250 m at 13 kHz). In addition to the diurnal phase shift, there are also phase shifts due to modal interference (particularly at night), due to long-path interference (particularly on East-to-West paths) and due to ionospheric disturbances (solar X-ray flames, solar proton precipitation, electron precipitation). These phase shifts cause bias errors in the estimates. The incorporation and estimation of bias errors in the phase rate model is discussed by Olson et al(ref.24). They find that bias errors of 0.5 ms^{-1} are typical.

One way to reduce the bias error due to ionospheric changes is to employ differential Omega, for which the base station as well as the sonde receives the Omega signal. If the sonde is not too far from the base station, less than about 50 km, then the changes in phase due to ionospheric movements are the same at both receivers, and may be removed by differencing the observed Omega phases at the sonde and the base station. Since the base station is at rest, the resulting observed changes in phase should be solely due to translation of the sonde. Although this technique removes the phase changes due to ionospheric movement, inasmuch as the changes at the sonde and base station are correlated, it does introduce the error which results from measuring phase of the Omega signal at the base station, and, as will be seen in the next section, this can be significant. A fuller discussion of differential Omega is given by Acheson(ref.25), Beukers(ref.26), Edgar(ref.27) and McKaughan(ref.28). The ionospheric changes which differential Omega is designed to deal with vary slowly with time and are large in extent. The errors due to rapid localised disturbances which are caused by solar flares, see for example Olson and Passi(ref.29), are not so readily removed by differential Omega.

5.2 Measuring phase

The first stage in the data analysis is to measure the phase of the received Omega signal. Aspects of necessary electronics and analysis methods are discussed by Afanasjevs(ref.19), Olson(ref.16,24), Govind(ref.14), Passi and Olson(ref.15).

It appears that the commonest method used to determine phase in Omega sondes is to time the zero crossing of the Omega signal with respect to the reference signal; the error in this method is discussed below. If the bandwidth of the input receiver is 6 Hz, then, at most, 6 uncorrelated measurements can be made per second. This is a fundamental mathematical relation which relates the highest frequency at which uncorrelated values of phase can be sampled to the receiver bandwidth. If the sampling frequency exceeds the bandwidth, the data become correlated and no further real information is gained. When we come to estimate rate of change of phase in Section 5.4 we shall see that accurate rate of phase change requires a fast sample rate, ie a wide bandwidth. This is opposite to the signal-to-noise requirement of a narrow bandwidth, so some compromise (designated an optimum solution) must be found. Although signal-to-noise ratio can be improved by reducing bandwidth, there is a limit to this because the lightning noise is impulsive, reducing the bandwidth to below about 50 Hz will produce ringing. Although receivers are designed to discriminate against these noise spikes, the problem still remains to some

extent.

The first step-up in sophistication for the determination of phase is to integrate the Omega signal in phase and in quadrature with the reference. This is generally done for the length of each Omega transmission, ie 1 s; by doing so the effective bandwidth is reduced to 1 Hz, with a consequent improvement in signal-to-noise ratio. But it means, from the argument above, that only one uncorrelated data point per second can be obtained. In the analysis below we will derive an expression for the phase error in terms of the effective signal-to-noise ratio over a 1 Hz bandwidth and the effective receiver bandwidth. Table 1, taken from Watt(ref.2) gives the measured VLF atmospheric noise at 10 kHz over a 1 Hz bandwidth, which is seen to vary between 4 and 40 μV/m. The larger values occur further North and in December through February. In comparison with this, Table 3 shows typical Omega signal strength in the Australian region to be in the range 20 to 1000 μV/m. The expected signal-to-noise ratio depends, of course, on the bandwidth and on the limiter (see Table 2).

We now proceed to relate the error in the measurement of phase to the signal-to-noise ratio. Figure 6 illustrates how the phase can be measured by timing zero crossings. The phase of the received Omega signal is compared with the phase of the stable oscillator at the base station. The phase is measured by counting a several megahertz clock during the interval between rising edge of the sampling clock (100 Hz in this case) and the next positive crossing of the Omega signal. The inset to the figure illustrates the error in measuring the phase of the zero crossing because of noise. Near the zero crossing the received signal is given by

$$S(t) = A\omega t + \sigma_n g_n \qquad (1)$$

where A = amplitude of the Omega signal voltage

ω = angular frequency of the Omega signal

σ_n = standard deviation of the noise voltage

g_n = unit variance Gaussian random variable

and we have made the approximation $\sin\omega t = \omega t$ near the zero crossing.

The phase error standard deviation is therefore given by

$$\sigma^2_{\emptyset} = \sigma^2_n/2A^2 = 1/2S \text{ (rad)}^2 \qquad (2)$$

where S is the signal to noise ratio. If we denote by $\sigma_{n.1}$ the noise standard deviation over a 1 Hz bandwidth, then we can show the dependence of phase error on the receiver bandwidth, b, explicitly by writing equation (2) as

$$\sigma^2_{\emptyset} = \sigma^2_{n.1}\, b/2A^2 = b/2\, S_1 \text{ (rad)}^2 \qquad (3)$$

Some typical measurements of phase are shown in figure 7. These data, each graph corresponding to 1 s of measured phases, were taken from Afanasjevs et al(ref.19). They were measured at 10 ms intervals (corresponding to a

bandwidth of 100 Hz, qv) from a balloon flight launched from a ship in the mid-Atlantic. The received signals from North Dakota were the strongest, and those from Norway and Trinidad the weakest. The dependence of the phase error standard deviation on the strength of the received signal is clearly shown. Note the presence of a large number of rogue points. A data processing filter which eliminates these points is essential.

In Table 4 we give values of phase error for several values of effective signal-to-noise ratio and bandwidth, calculated using equation (3). We see that the data in figure 7, which were taken with a 100 Hz bandwidth and had RMS phase error of about 20°, would have had an effective SNR over 1 Hz bandwidth greater than 200.

5.3 Estimating rate of change of phase

There are two ways in which the sonde velocity can be derived from the measured phase data:

- the sonde position can be calculated for each block of phase data, and velocity determined from rate of change of position.
- the rate of change of phase is determined, and velocity calculated from the rate of change of phase.

The latter method is generally used, largely because the analysis is more accurate. In determining the rate of change of phase, assumptions must be made as to whether the change is linear, quadratic or cubic with time. Also it must be decided whether to allow for drift and bias in the measurements caused by drift and bias in the reference oscillator (and in the received signal due to ionospheric changes). These problems are discussed by Olson et al(ref.24), Passi(ref.30), and Govind(ref.14).

We will start by assuming that the phase varies linearly with time. The variance in the estimate of the rate of change of phase is then related to the variance of phase by the standard formula

$$\sigma^2_{\dot{\phi}} = \sigma^2_{\phi}/\Sigma(t_i-t)^2 \ (\text{rad/s})^2 \qquad (4)$$

If the data consist of N uncorrelated points spaced at intervals Δt, so that data spans a total time $T = N\Delta t$ this can be written as

$$\sigma^2_{\dot{\phi}} = 12\sigma^2_{\phi}/\{T^2(N^2-1)\} \ (\text{rad/s})^2 \qquad (5)$$

$$\approx 12\sigma^2_{\phi}/\{T^2N\}$$

$$\approx 12\sigma^2_{\phi}\Delta t/T^3 \qquad (6)$$

As we discussed earlier, the maximum sampling rate at which we will get uncorrelated samples is the Omega receiver bandwidth, ie $\Delta t = 1/b$.

We now wish to relate the variance of rate of change of phase to the primary variables of concern, that is, to the signal-to-noise ratio and the input bandwidth. We do this by substituting equation (3) into equation (6)

which gives

$$\sigma^2_{\dot{\phi}} = 60/S_1T^3 \text{ (rad/s)}^2 \quad (7)$$

Although bandwidth drops out of the final expression, the choice of bandwidth deserves careful attention in the receiver design, if only because it ultimately determines whether phase can be measured at all. Some of the problems relating to choice of bandwidth have been alluded to earlier. The extra factor of 10 in equation (7) is required because the transmission from each station is only 1 s in 10, so that data is effectively reduced by a factor of 10 (this is only approximate, and neglects the benefits of phase locked loops).

We see that the effects of bandwidth in receiver noise and in the sampling time cancel, and the variance in the measured rate of change of phase is inversely proportional both to the signal-to-noise ratio and to the total time over which the phase samples were taken.

This analysis assumed that the phase changes linearly with time. Because the wind profile does not change linearly with attitude, this assumption is not valid and will add to the error in the estimate of phase. Passi(ref.30,31) and Govind(ref.14) discuss this problem. The first refinement which they propose is to assume that the variation with time is not linear but quadratic. This gives some improvement, but does not model the physical fact that the phase varies in a continuous manner. The mathematical tool which fulfills this requirement is the spline fit, and it has been found that a cubic spline fit to the phase data is admirable. Figure 8, taken from Govind(ref.14) gives an example of phase data fitted by cubic spline. The rate of change of phase is given by the slope of the curve at the given time.

Analysis of the error in estimating rate of change of phase using quadratic time dependence or a cubic spline fit give the same parameter dependence as for the linear fit, equation (6), except for different numerical factors. Therefore it is convenient to generalise equation (7) for smoothing routines other than linear by multiplying by a factor, r, less than unity, called the phase slope variance factor, which parameterises the reduction in error which results from using sophisticated curve fitting instead of linear regression in fitting the phase data

viz

$$\sigma^2_{\dot{\phi}} = 60r/S_1T^3 \text{ (rad/s)}^2 \quad (8)$$

Empirical values derived from analysing real data give $r \sim \frac{1}{2}$ using quadratic regression in place of linear, and $r \sim \frac{1}{4}$ using cubic spline fit in place of linear regression. This shows that there is considerable advantage in using sophisticated techniques in fitting the phase data. Using a cubic spline, or perhaps an even more powerful optimisation technique, to full advantage requires all the data to be assembled before processing starts. Given the power of modern microprocessors, this is not seen as difficult.

5.4 Calculating the wind profile

The last stage in the data analysis is to convert the measured phase rates to velocities Northward and Eastward. Methods for accomplishing this are

discussed by Olsen et al(ref.24), Passi(ref.32,33), Govind(ref.34,35) Acheson(ref.25), Passi and Olson(ref.15); we will do no more here than give a resume of the method as a preparation for obtaining expression for wind variances in terms of phase rate variances.

Let the absolute phase of the Omega signal at the receiving sonde from transmitter j be given by

$$p_j = (2\pi R/\lambda) f_j \tag{9}$$

where R = radius of the earth

λ = wavelength of the Omega VLF

f_j = angle subtended by the transmitter and sonde at Earth's centre

If η,ξ = latitude and longitude of sonde and transmitter, then

$$\cos f_j = \cos(\xi_i - \xi)\cos\eta\cos\eta_i + \sin\eta\sin\eta_i \tag{10}$$

The measured quantity, ϕ_j, is given by

$$\phi_j = p_i - p_L + e_j \tag{11}$$

Where p_L is the phase of the local oscillator at the base station and e_j is the error in measuring phase. Three transmitters are necessary to give a position fix, four or more transmitters give a redundancy which, in general, improves the accuracy.

As illustrated in figure 4, the first step in finding position, and therefore velocity, is to find the relative phase of the received transmitter signals. We choose one of the transmitters, m, as the reference, and express the phases of the others with respect to this:

$$\phi_{jm} = p_j - p_m = \phi_j - \phi_m + e_{jm} \tag{12}$$

The phase of the local oscillator drops out. If we substitute equation (9) into equation (12), and differentiate with respect to time we get the following expression for phase rate in terms of the North and East components of the sonde

$$\dot{\phi}_{jm} = \left(\frac{2\pi}{\lambda}\right)\left[\frac{1}{\cos\eta}\cdot\frac{\partial f_{jm}}{\partial\xi}\cdot V_E + \frac{\partial f_{jm}}{\partial\eta}\cdot V_N\right] + e_{jm} \tag{13}$$

where $V_E = R\cos\eta\,\partial\xi/\partial t$,

$V_N = R\,\partial\eta/\partial t$

If we define the column vector $\dot{\phi} = \{\dot{\phi}_{im}, \ldots\ldots \dot{\phi}_{km}\}$, and similarly e, and the kx2 matrix, with its i'th row having elements

$$F_{i1} = (2\pi/\lambda\cos\eta)\partial f_{im}/\partial\xi$$

$$F_{i2} = (2\pi/\lambda)\partial f_{im}/\partial\eta$$

we can rewrite equation (12) as the matrix equation

$$\dot{\phi} = F V + e \tag{14}$$

The minimum variance unbiased estimator, $\hat{V}$, of the velocity, V, is then given by

$$\hat{V} = (F' \Sigma_{\dot{\phi}}^{-1} F)^{-1} F' \Sigma_{\dot{\phi}}^{-1} \dot{\phi} \tag{15}$$

where the prime denotes transpose of the matrix.

$\Sigma_{\dot{\phi}}$ is the covariance matrix of the phase rate difference vectors, and is given in terms of the phase rate variances we calculated in the last section, by

$$(\Sigma_{\dot{\phi}})_{jm} = (\sigma^2_{\dot{\phi}})_j + (\sigma^2_{\dot{\phi}})_m \tag{16}$$

The covariance matrix of the velocity is given by

$$\Sigma_V = (F'\Sigma_{\dot{\phi}}^{-1} F)^{-1} \tag{17}$$

Equation (17) gives us a formal expression for the errors of derived velocity in terms of the errors in the measured values of phase rate. Extensive calculations using this expression have been carried out by Passi(ref.30), Olson(ref.36) and by Olson et al(ref.24). The last of these is a most valuable document. Taking the paper of Olson(ref.36) as its starting point, it calculates world-wide the RMS error in wind using Omega. The calculations include estimates of VLF noise, VLF signal propagation, phase variance models and the geometrical dilution of precision. The computations in effect follow the same path as we have done, but whereas we have obtained simple analytical expressions to determine what parameters effect the wind error, he has included all effects in detail to calculate actual RMS wind errors. His results are shown as curves of equal wind error plotted on a map of the earth. They refer to four minute averaging of the data, and assume a phase slope variance factor of 1/3. An example of his results is given in figures 9(a) and 9(b) - which are for the Australian Omega station not operational and operational respectively, other figures show the calculated wind error due to bias. These figures and the associated tables, which were computed for various combinations of Omega transmitters, are extremely valuable, and should be referred to.

Although these figures and tables go a long way to fulfilling the requirements of this study, they do not enable a direct estimate to be made of the importance of signal to noise ratio and averaging time on the wind estimate error. For that end we will continue on the path of simplification which we have used hitherto. As explained in Section 2, the

maximum position accuracy occurs when the hyperbolae of constant phase from different sets of transmitters intersect normally, and that degradation from that optimum is parameterised by the factor known as geometric dilution of precision. Equation (17) contains all this in a rigorous formal manner, but for our purposes is sufficient to get an estimate of how the transmitter sites relate the phase rate and velocity variances. An equation suitable for our purposes, given by Govind(ref.14) is

$$\sigma^2_v = \frac{\sin^2 \tfrac{1}{2}(\psi_A-\psi_B) + \sin^2 \tfrac{1}{2}(\psi_C-\psi_D)}{\sin\tfrac{1}{2}(\psi_A-\psi_B)\,\sin\tfrac{1}{2}(\psi_c-\psi_D)\,\sin[\tfrac{1}{2}(\psi_A+\psi_B) - \tfrac{1}{2}(\psi_C+\psi_D)]} \cdot \left(\frac{\lambda\sigma_{\dot\phi}}{2\pi}\right)^2 \quad (18)$$

where the ψ's are the bearing angles to the transmitters at the sonde, paired as A-B, C-D but not all necessarily distinct, eg A can be the same as C. The factor involving the sines is always greater than 2, this minimum occuring when the pairs sites are normal to each other. In Table 5 we give values of this factor for four sites in Australia and three Omega transmitters. The table is included to give an indication of the range of the factor. In an actual situation, the receiver would use data from as many Omega stations as possible, given the constraint that the increase in accuracy obtained by using another station is not more than outweighed by that station having very poor phase accuracy.

By representing the GDOP by a factor f, from equation (8) we have the following expression for velocity error.

$$\sigma^2_v = 60fr(\lambda/2\pi)^2/S^1T^3 \quad (19)$$

We have calculated velocity error as a function of effective signal-to-noise ratio over a 1 Hz bandwidth and smoothing time using equation (19), and presented the results in Table 6. We see that to get errors less than 2 ms^{-1} we need a smoothing time of 2 min for an effective SNR of 200, and SNR of 20 for 4 min.

6. OMEGA WIND SONDE EXPERIMENTS

In Table 7 we have collated the information we have been able to obtain, from a reading of the literature, on results of experiments using Omega sondes to measure the wind profile. We have compiled the list under the Author of the report in alphabetical order, and have included in the table the main parameters of interest: wind error, averaging time, descent rate etc. Although this data is most valuable, it is frustrating that much of the data which would be of interest to us, for example signal-to-noise ratio and bandwidth, is not given in the Reports.

We found it curious how the accuracy appears to be in the range 1 to 3 ms^{-1} for such a wide set of conditions. The results of the last section would suggest a much greater range of errors, given the wide variation in signal to noise ratios, S_1, phase slope variance factors, r, and geometrical dilutions of precision, f, which there would have been. For some reason they all appear to cancel out in the wash.

For more details on the results of the experiments it is best to go to the original papers. We will examine only one set of data, that of Olson et al(ref.24), because it gives details on phase accuracies and because Olson conducted some experiments at Darwin and Perth, albeit for stationary receivers. The stationary receiver was used as a last resort when there was

no tracking radar to measure winds to compare with the Omega winds. However, since the system was a complete Omega sonde system, the apparent winds give a good indication of the wind errors which would occur in a drop.

Table 8 presents the phase error data which Olson et al(ref.24) observed at Perth and Darwin, for the signals from the various Omega transmitters. From this data we have calculated the signal-to-noise ratio which would produce this phase error, using equation (2). Below the data we give the phase error which they predicted from a model they developed. The predictions are in fair agreement with the data. Finally, we give the extremes of signal-to-noise ratio, calculated using the data we have obtained in Tables 1 and 3, for a 1 Hz bandwidth. We have included a factor of 3 improvement of SNR due to clipping. Although Olson does not make it clear in his report whether his signals are clipped, the fact that he discusses the matter suggests that they are. It will be seen that there is good agreement between Olson's measurements and the detailed calculations he makes of SNR using his complete model. There is also fair agreement with our simple estimates using the methods described in the text. This means we can use them as an estimate for wind errors with some confidence.

7. SUMMARY

We now collect together the contributions to the wind error using Omega which were discussed in Section 5. The first error source to be examined is the change in phase at the receiver due to changes in the ionosphere. There is a regular diurnal pattern which can be calibrated out, but superposed on this are both variations in the diurnal pattern and more rapid changes (see figure 1). Since we are interested in determining sonde velocity it is only uncalibrated variations in the change of phase; a given uncalibrated rate of change produces a bias error in the final estimated velocity. This produces a bias which can be estimated (Olson et al, reference 24). Alternatively the bias can be overcome by using differential Omega which removes errors due to uncalibrated ionospheric changes. However it adds the error in measurement of the reference Omega phase at the base station. Also, it is unlikely that differential Omega will cope with the major ionospheric disturbances produced by solar flares.

The next source of error which needs to be discussed is the error in the measurement in the phase of the Omega signal due to atmospheric VLF noise. This noise is produced by lightning strikes. Table 1 gives expected values for the atmospheric VLF noise at 10 kHz due to world wide thunderstorm activity, expressed in microvolts per metre over a 1 Hz bandwidth. As discussed in the text, if the IF bandwidth is much less than 100 Hz the impulsive nature of the noise produces ringing. For a 100 Hz bandwidth the data in Table 1 must be multiplied by a factor of 10, which, when compared with the signal strengths of the Omega signals (see Table 3) gives a signal to noise ratio less than one. However, because of the impulsive nature of the noise, its probability distribution is highly skewed and clipping of the received signal can improve the signal-to-noise ratios by a factor of at least three (see Table 2).

When the effective signal-to-noise ratio is greater than about ten the phase can be determined by measuring the zero crossing. Otherwise, the phase can be determined by multiplying the signal in phase and quadrature and integrating over a time Δt. This is done, for example, by Olson(ref.16) and Edgar(ref.27), and is equivalent to reducing the bandwidth to $1/\Delta t$. Providing that the signal-to-noise ratio is high enough to measure phase at all, the phase variance is related to the signal-to-noise ratio by

$$\sigma^2_\phi = 1/2S = b/2S_1 \text{ (rad)}^2$$

where S_1 is the signal-to-noise ratio for a 1 Hz bandwidth and b is the receiver bandwidth.

As explained in the text, although reducing the bandwidth increases the signal to noise ratio, and hence reduces the error in measuring phase, the number of independant samples of phase which can be taken per second reduces with increasing bandwidth. For a bandwidth, b, the minimum time between samples before they become correlated is 1/b. This has an impact on the next stage of the data analysis, which is to estimate the rate of change of phase from the phase measurements. As shown in the text, the phase rate variance is related to phase variance by

$$\sigma^2_{\dot\phi} = 6r(\sigma^2_\phi/n)(\tau/T^3)$$

where T is the observation time (which we have called the averaging time), τ is the interval between Omega transmissions (=10 s), n is number of phase samples in each 1 s Omega transmission and r is the phase slope variance factor, which depends on the method of fitting a curve to the data. For a cubic spline $r = \frac{1}{2}$.

Finally, we must convert phase rates to velocity North and East. The relationship is essentially a geometrical one, which depends on the azimuths of the Omega transmitters with respect to the receiver. The factor which represents this relationship is analogous to the geometrical dilution of precision which is used is standard Omega position location, and will be represented by f.

ie

$$\sigma^2_V = f(\lambda\sigma_{\dot\phi}/2\pi)^2 (ms^{-1})^2$$

For four transmitters optimally placed, ie in quadrature, with the receiver at the centre, f = 2. Typical values in Australia are given in Table 4 and show that f lies between 2 and 12.

Combining the above equations, and noting that the maximum number of phase measurements which can be made in 1 s is 1/b, we have finally

$$\sigma^2_V = 6rf\tau(\lambda/2\pi)^2/S_1T^3$$

substituting τ = 10 s, λ = 22.1 km at 13.6 kHz gives

$$\sigma_V = 2.7\times10^4\sqrt{rf/S_1T^3}\ ms^{-1} \qquad (20)$$

We see that the standard deviation in wind varies inversely with the square root of the signal-to-noise ratio (taken over a 1 Hz bandwidth) and with the total observation time to the three halves. Note that it does not depend on the receiver bandwidth. The results of calculations using the above equation, with rf = +1, are given in Table 5.

Given a desired measured wind accuracy, equation (20) enables the averaging time to be calculated as a function of the expected SNR. This time interval then must be compared with the desired descent rate of the sonde, taking into account the assumed and actual form of the wind profile. To explain what we mean by this, we take an example. Suppose we fit the phase data to a cubic spline (which, as discussed in Section 5.3, gives small phase variance), then, if the wind profile over the altitude interval through which the sonde falls in the averaging time can indeed by approximated by a cubic, the estimate of the velocity profile from the data analysis will be good. This is true no matter how long the averaging time be. Therefore, given the order of the fitting polynomial (in this case cubic) we examine typical wind profiles and decide on the maximum altitude range over which the profile can be fitted by that polynomial, with the accuracy desired for the wind determination. The averaging time is the time taken for the sonde to descend through this altitude. In any given situation a compromise must be found between the conflicting demands of a fast descent rate, a long averaging time, and the maximum altitude range over which the wind profile can be approximated by a cubic within the desired accuracy of velocity.

In addition to the reports referenced in the text, we came across a number of references to Omega sonde reports which we were not able to obtain. For the reader wishing to follow the matters discussed in this Memorandum further, we recommend he go first to the papers of Govind(ref.14,17) and of Olson et al(ref.24) which between them give an excellent description of the Omega wind finding system, data analysis and estimates of error. A discussion of results of recent Omega sonde drops from aircraft is given by Julian(ref.43) and Franklin(ref.44).

8. ACKNOWLEDGEMENTS

I am most grateful for valuable discussions with R.S. Edgar of Radio Group, K.J.W. Lynn of Navigation Group, and with E. Jesson of the Bureau of Meteorology, Melbourne.

NOTATION

A	amplitude of Omega signal (volt per metre)
b	bandwidth of Omega receiver (Hertz)
e	error in measuring phase of Omega signal
f_i	angle subtended by Omega transmitter and sonde at earth's centre
f	factor by which velocity variance is increased due to geometrical dilution of precision.
p	absolute phase of received Omega signal
R	radius of earth
r	phase slope variance factor (factor by which error in estimate of phase slope is reduced by using sophisticated curve fitting in place of linear regression)
n	number of Omega samples measured in each 1 s Omega transmission
N	number of Omega phase samples used in computing rate of change of phase of Omega signals.
S	signal-to-noise ratio at Omega receiver
S_1	= S for receiver bandwidth of 1 Hz
Δt	sampling interval of Omega phase measurements (second)
t	time (second)
t_i	time of i^{th} sample
T	averaging time over which one set of samples of Omega phase data is taken in smoothing (second)
λ	wavelength of Omega radiation
σ_n	standard deviation of VLF noise (volt per metre)
σ_ϕ	standard deviation of measured Omega phase (radian)
$\sigma_{\dot{\phi}}$	standard deviation of estimated rate of change of phase
ϕ	phase of Omega signal relative to reference (radian)
η, ζ	latitude and longitude
ω	angular frequency of Omega signal
Σ	covariance matrix
ψ	bearing angle of transmitter at receiver

τ	time interval between successive Omega transmissions (= 10 s)
GDOP	geometrical dilution of precision

REFERENCES

No.	Author	Title
1	Beukers, J.M.	"A review and applications of VLF and LF transmissions for navigation and tracking". Navigation 21, 117, 1974
2	Watt, A.D.	"V.L.F. Radio Engineering". Pergamon Press, 1967
3	Galejs, J.	"Terrestrial propagation of long electromagnetic waves". Pergamon Press, 1972
4	Budden, K.G.	"Radio waves in the ionosphere". C.U.P., 1961
5	Burgess, R. and Jones, T.	"The propagation of l.f. and v.l.f. radio waves with reference to some system applications". Radio and Elect. Eng. 45, 47, 1975
6	Morris, P.B.	"Omega propagation corrections: background and computational algorithm". ONSOD-01-74. Department of Transport, 1974
7	Kaspar, J.F.	"Omega : global navigating by VLF fix". IEEE Spectrum, p 59, May 1979
8	Thompson, A.D.	"Omega system performance predictions". Navigation, 24, 304, 1977
9	Hogle, L., Markin, K. and Toth, S.	"Evaluation of various navigation system concepts". ARINC Res. Corp. FAA-EM-82-15, 1982
10	Lynn, K.S.W.	Private communication
11	Swanson, E.R.	"Omega envelope capability for lane resolution and timing". Naval Elect. Lab. Center, San Diego, 1973
12	-	"Windsonde WS 80-15". Vaisala OY, Helsinki, Finland
13	-	"Instruction manual for CORA automatic sounding system aerological parameters computation program". Vaisala OY, Helsinki, Finland, 1979
14	Govind, P.K.	"Omega windfinding systems". J. Appl. Met. 14, 1503, 1975

No.	Author	Title
15	Passi, R.M. and Olson, M.L.	"Carrier balloon windfinding subsystem evaluation". Bull. Amer. Met. Soc. 55, 1463, 1974
16	Olson, M.L.	"Superpressure balloons and communications satellites - a new approach for tropical meteorological soundings". IEEC Trans. on Geosci. Elect. GE-13, 1, 60, 1975
17	Govind, P.K.	"Dropwind sonde instrumentation for weather reconnaissance aircraft". J. Appl. Met. 14, 1512, 1975
18	Poppe, M.C.	"Lo-cate III - the application of retransmitted Omega to the tracking of remote objects". 1st Omega Symp., Am. Inst. Nav., 1971
19	Afanasjevs J., Levanon, N., Ellington, S.D. and Oehlkers, R.A.	"Raw data digitising and recording system for the Omega-sonde wind finding station". IEEE Trans. on Geosci. Elect. GE-13, 4, 158, 1975
20	Morrissey, J.F. and Weiss, D.B.	"Dropsonde wind measurements using Omega/Loran tracking". AFCRL-TR-75-0096, 1975
21	Reeves, R., Williams, S., Rasmusson, E. and Acheson, D.	"GATE connection subprogram data centre - analysis of rawinsonde intercomparison data". NOAA Tech Rept. EDS 20, 1976
22	-	"RPV Omega navigation system". Develco Inc, California, USA
23	Fraser, E.C., Marsh, J.L. and Rorden, L.H.	"Omega navigation of RPVs". Develco Inc, Sunnyvale, California
24	Olson, M.L., Passi, R. and Schumann, A.	"Omega wind error estimation". NCAR Tech Note - 13+EDD, 1978
25	Acheson, D.T.	"Omega windfinding and GATE". Bull. Amer. Met. Soc. 55, p 385, 1974, GARP Topic No. 33
26	Beukers, J.M.	"Accuracy limitations of the Omega navigation system employed in the differential mode". Navigation 20, 81, 1973

No.	Author	Title
27	Edgar, R.S.	"The application of differential Omega to land navigation within Australia". ERL-0129-TM, 1980
28	McKaughan, M.E.	"Summary of investigations of a differential Omega system". 1st Omega Symp., Am. Inst. of Nav. p 120, 1971
29	Olson, M.L. and Passi, R.M.	"Error estimation of Omega-derived wind measurements". IEEE P.L.A.N.S., p 359, 1978
30	Passi, R.M.	"Errors in wind measurements from Omega signals". NCAR-TN/STR-88, 1973
31	Passi, R.M.	"Smoothing improvement factor in Omega wind errors". J. Applied Met. 16, 735, 1977
32	Passi, R.M.	"Wind determination using Omega signals". J. Applied Met. 13, 933, 1974
33	Passi, R.M.	"On some aspects of Omega wind finding". J. Appl. Met. 14, 1499, 1975
34	Govind, P.K.	"Dropsonde velocity measurements based on Omega signals". Atmos. Tech. 2, p 39, 1973
35	Govind, P.K.	"Velocity computations from radio range measurements". IEEE Trans. of Aerosp. & Elect. Sys. AES-10, 5, 636, 1974
36	Olson, M.L.	"Central Pacific VLF signal survey and Omega wind error predictions." NCAR Tech Note - 120+EDD, 1977
37	Acheson, D.T.	"Omega wind-finding capabilities - Wallops Island experiments". NOAA Tech Memo. EDS CEDDA-1, 1973
38	Loitiers, B. and Brosson,	"Des signaux de radio navigation Omega pour measurer le vent". La Meteorologie, p 71, November 1975
39	Weiss, B.D. and Morrissey, J.	"Investigations into utilisation of Loran and Omega wind-finding systems for measuring winds below an aircraft". AFCRL-72-0399, 1972

No.	Author	Title
40	Simpson, R.H., Govind, P.K. and Holle, R.	"The GATE dropwind sonde program". Bull. Am. Met. Soc. 56, 984, 1975
41	Nybo, L.W.	"Omega windfinding system designed to meet accuracy requirements of GARP Atlantic tropical experiment". Bull. Amen. Met. Soc. 54, 926, 1973
42	Denbigh, P.H.	"Techniques and errors of balloon location by low-orbit meteorological satellites". J. Brit Interplanet Soc 23, 409, 1970
43	Julian, P.R.	"The aircraft dropwindsonde system in the global weather experiment". Bull. Amer. Meteorol. Soc. 73, 619, 1983
44	Franklin, J.	"Omega dropwindsonde processing". NOAA Tech Memo ERL AOML-54, 1983

TABLE 1. EXPECTED ATMOSPHERIC NOISE AT 10 KHZ

The data are given in microvolts per metre over a 1 Hz bandwidth

LST	0300	0700	1100	1500	1900	2300
Spring	16	16	10	14	16	16
Summer	22	18	18	36	40	28
Autumn	14	13	9	11	16	16
Winter	10	10	5	5	5	9

(a) Darwin data from CCIR322 (Watt, reference 2)

Darwin	Brisbane	Hobart	Perth
40	32	16	20

(b) Comparison of expected noise at four sites in Australia. Worst case, viz Summer evening.

NB. The noise is due to lightning discharges and is therefore impulse, with a skewed probability distribution containing a large number of high values. Therefore a limiter in the receiver will give a significantly larger effective signal-to-noise ratio.

TABLE 2. REDUCTION IN VLF NOISE BY CLIPPING

$a_c/\bar{a}$	0.5	0.7	1.0	2.0	5.0	10.0
$\bar{a}_c/\bar{a}$	0.06	0.2	0.3	0.6	0.8	0.9

$\bar{a}$ = mean VLF noise

a_c = amplitude at which signal is clipped

$\bar{a}_c$ = mean VLF noise for clipped signals

Table calculated from VLF noise amplitude distribution function given by Galejs(ref.3).

TABLE 3. OMEGA SIGNAL STRENGTH

Data are given in microvolts per metre. Where significant mode mixing occurs, data are given in brackets. Data given in pairs: day, night

	Darwin	Brisbane	Hobart	Perth
Hawaii	45,30	63,36	28,25	10*,32*
LaReunion	70,220	35,180	50,200	180,350
Australia	450,(350)	1000,[1400]	-	560,[800]
Japan	200,280	71,200	40,126	60,180

* Liberia

TABLE 4. OMEGA PHASE MEASUREMENT ERROR

Table gives RMS error in a single phase measurement, in degree.

b	τ	S_1 = 10	20	50	100	200
0.1	10	4	3	2	1.3	0.9
1	1	13	9	6	4	3
10	0.1	42	30	19	13	9
100	0.01	-	-	60	40	30

b = input bandwidth (Hertz)
τ = equivalent integration time (second)
S_1 = signal-to-noise ratio for 1 Hz input bandwidth.

TABLE 5. GEOMETRICAL DILUTION OF PRECISION

The table gives the factor f (see equation (18)) by which wind error is degraded due to geometrical dilution of precision for combinations of three transmitters. Inclusion of the Australian station significantly improves the GDOP for Perth.

Re = Reunion, Ha = Hawaii, Ja = Japan

	Darwin	Brisbane	Hobart	Perth
Re-Ha, Re-Ja	4	5	6	14
Re-Ha, Ha-Ja	3	6	7	10
Re-Ja, Ha-Ja	2	3	3	24

TABLE 6. OMEGA VELOCITY ERRORS

Table gives estimated RMS velocity error in ms^{-1} using equation (19), and taking rf = 1.

S_1	T = 60	120	180	240
10	18	7	4	2
20	13	5	3	1.5
50	8	3	1.5	1.0
100	6	2	1.0	0.8
200	4	1.5	0.8	0.5

T = time over which one set of samples of Omega phase data is taken (second)

S_1 = effective signal-to-noise ratio over 1 Hz bandwidth

TABLE 7. OMEGA WIND SONDE EXPERIMENTS

Author	Ref	Date	Location	Error (ms^{-1})	Averaging time (min)	Balloon, parachute descent rate ms^{-1}
Acheson	37	Dec 72	Wallops	1.5,1.0,0.5	1,2,4	Met. balloon, 4
Govind	14,34	Jun 74	Canaveral	1.5	3	Parachute
Loitiers	38	?	?	2	?	Met. balloon
Morrissey	20	Apr 74	Kennedy	4-7,1-5	2,3	Parachute, 16 min from 6.7 km
Nybo	41	Dec 72	Wallops	1.5,1.3,1.0	1,2,4	Met. balloon
Olson et al	24	? 75	Kourou	1.3-3.3	4	Parachute
		Feb 76	Majuro	0.9-3.9	4	Parachute
		Mar 77	Diego Garcia	1.2-3.3	4	Parachute
		Mar 77	Clark AFB	1.5-3.6	4	Parachute
Passi	32	Oct 73	Wallops	~1	5	Parachute
Passi et al	15	Oct 73	Wallops	2.5,1.5,1.0	1,2,4	Parachute, ~27 at 22 km
Reeves et al	21	- 74	Cape Verde	1-3	1-4	Balloon
Weiss et al	39	Aug 71	Kennedy	4.0,2.5,1.5	1,2,4	Parachute, 12 to 30

TABLE 8. COMPARISON OF ESTIMATED AND MEASURED OMEGA PHASE ERRORS

The table compares the data and model predictions taken from reference 24 with simple estimates made in this report.

		Liberia	Hawaii	Reunion	Japan
Darwin:					
Observed residual noise, expressed as phase error (degree)	min	5	11	3	2
	max	15	29	5	4
SNR which would produce this phase error	max	70	14	180	410
	min	7	2	65	102
Model prediction of phase error (degree)		33	31	5	3
Equivalent SNR ($S = 1/2\sigma_\phi^2$)		1.5	1.5	65	180
Range in expected SNR from Tables 1 and 2, over 1 Hz bw	max	-	27	135	165
	min	-	3	6	15
Perth:					
Observed residual noise, expressed as phase error (degree)	min	4	10	1	3
	max	19	10	3	6
SNR which would produce this phase error	max	102	17	1500	180
	min	4.5	35	180	45
Model prediction of phase error (degree)		16	5	1.5	4
Equivalent SNR		7	65	750	100
Range in expected SNR from Tables 1 and 2, over 1 Hz bw *	max	18	-	180	90
	min	1.5	-	18	9

* We have included a factor of 3 improvement in SNR assuming the signal is clipped (see Table 2).

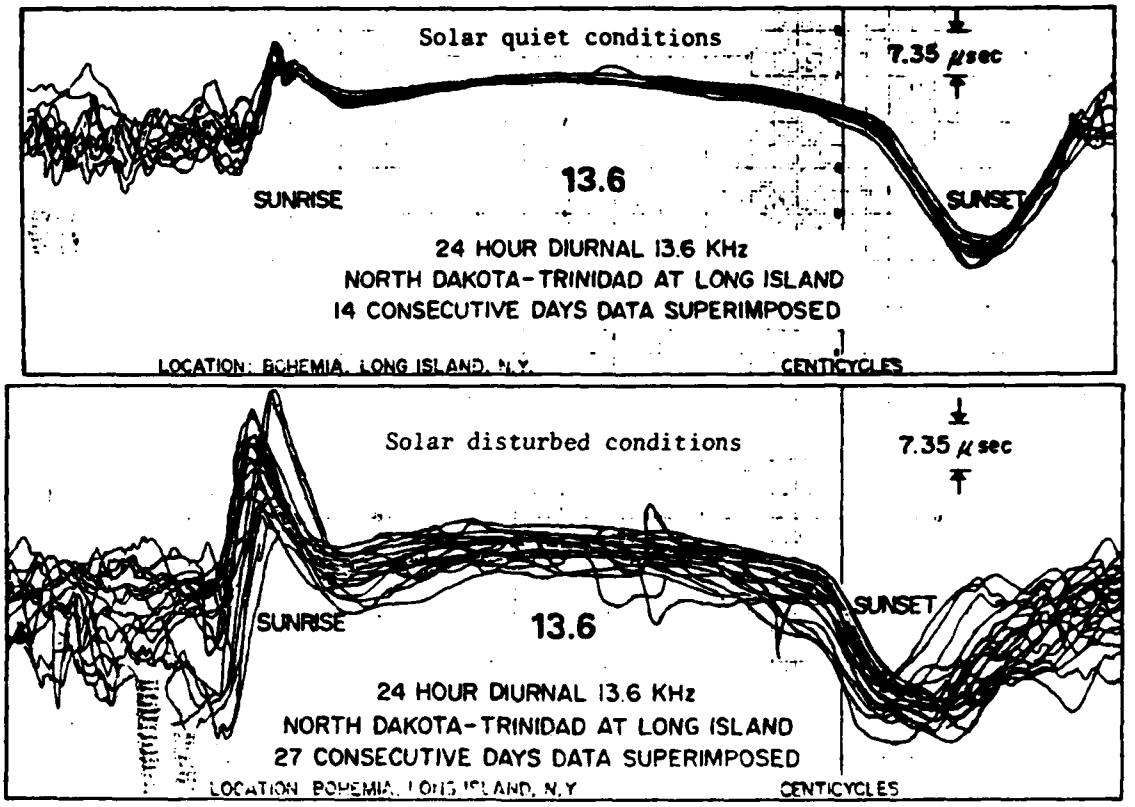

The figures show variation in the phase of the received Omega signal due to changes in the ionosphere. Taken from Beukers(ref.1).

Figure 1. Diurnal Omega phase differences

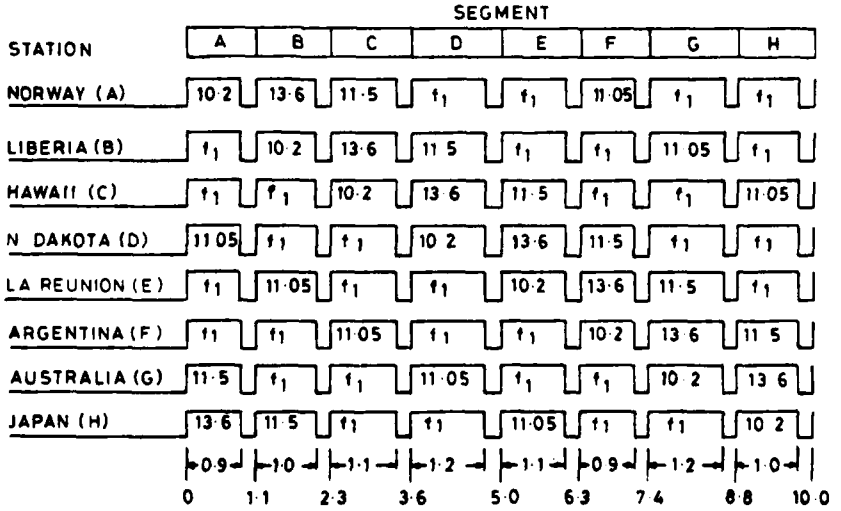

Figure 2. Omega signal transmission format

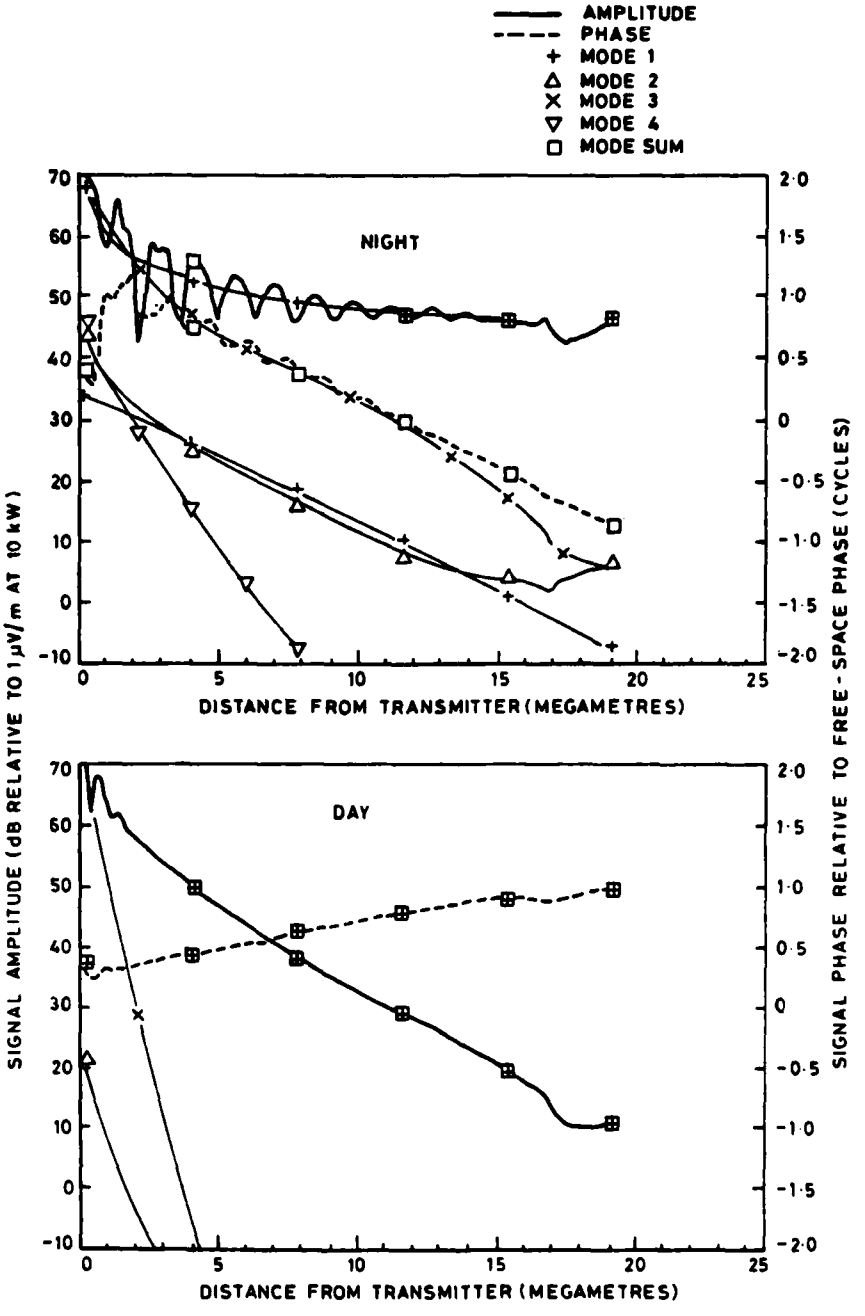

Figure 3. Omega signal strength vs distance

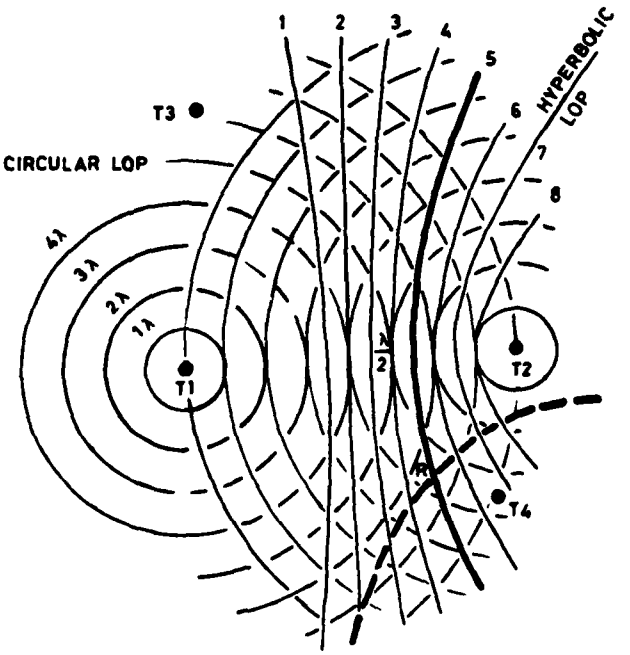

Figure 4. Hyperbolic navigation

The figure illustrates how the position of the receiver, R, is determined by intersection of constant-phase hyperbolae from the pairs of transmitters. In practice, position is found by taking phase differences from one site, and solving by matrix inversion, see text.

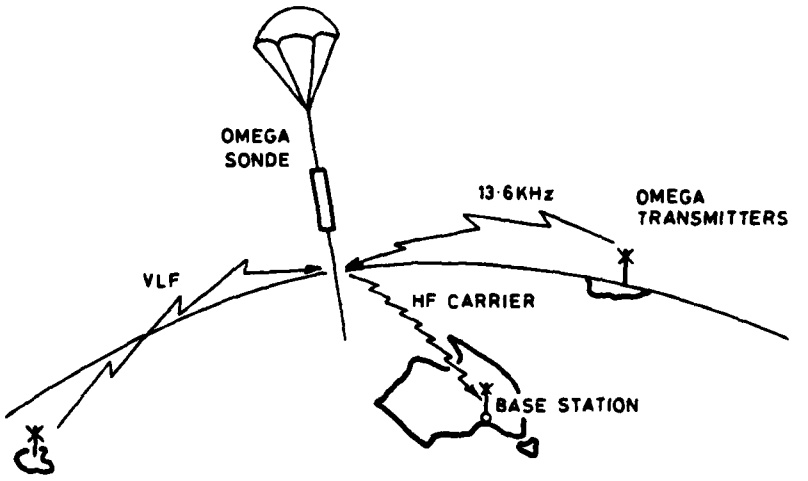

Figure 5. Scheme for using Omega sonde

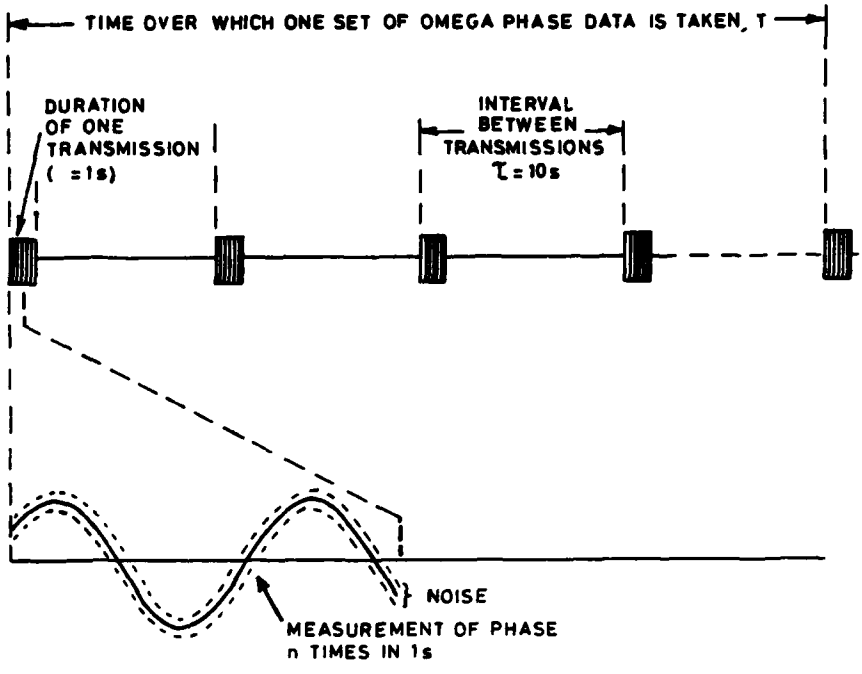

The figure illustrates the measurement of phase by zero crossing.

Figure 6. Omega signal phase measuring

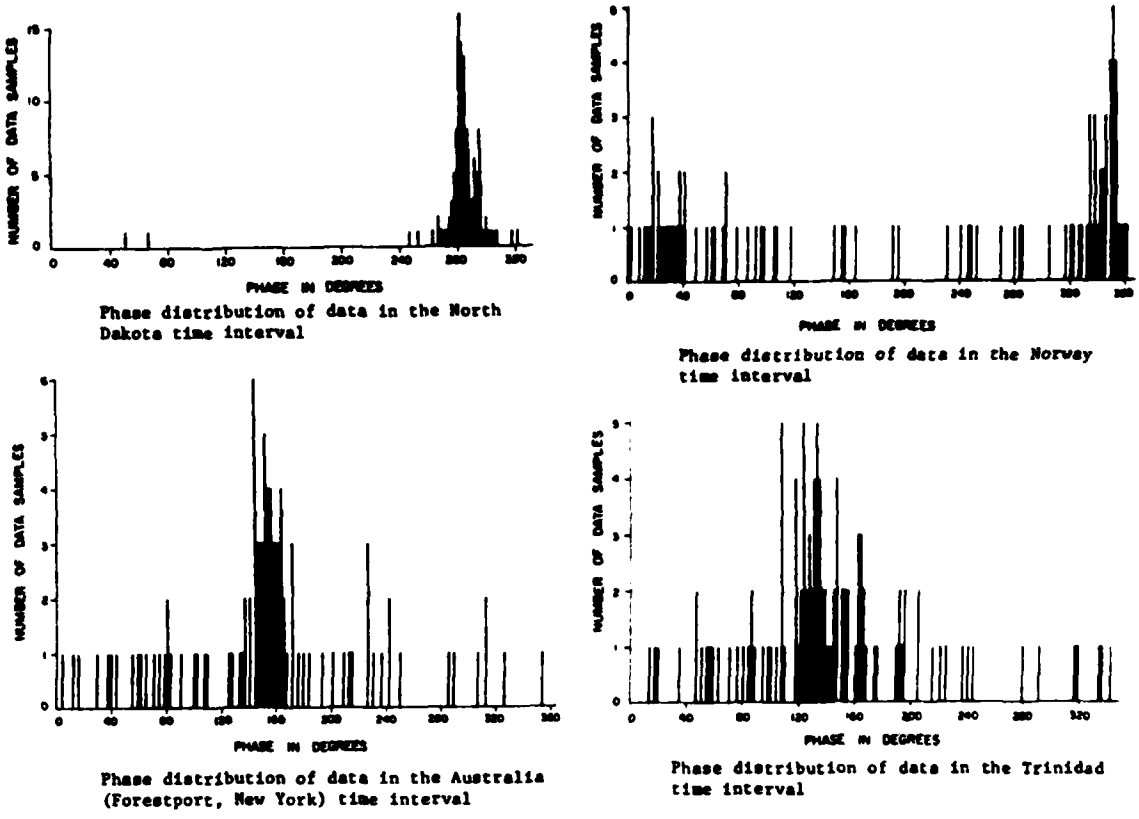

Figure 7. Typical measured Omega phase data

Taken from Afanasjevs, et al(ref.19).

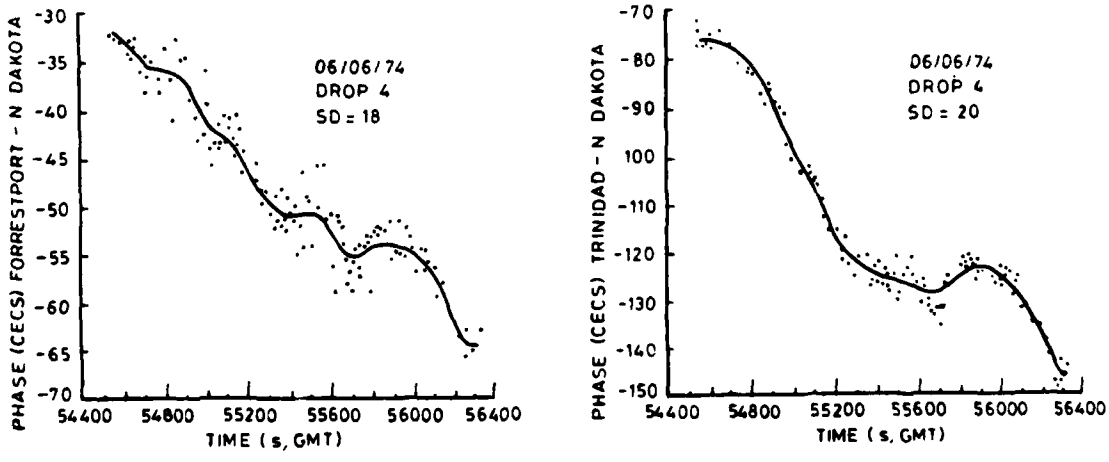

Figure 8. Cubic spline fit to a series of Omega phase data

Taken from Govind(ref.14).

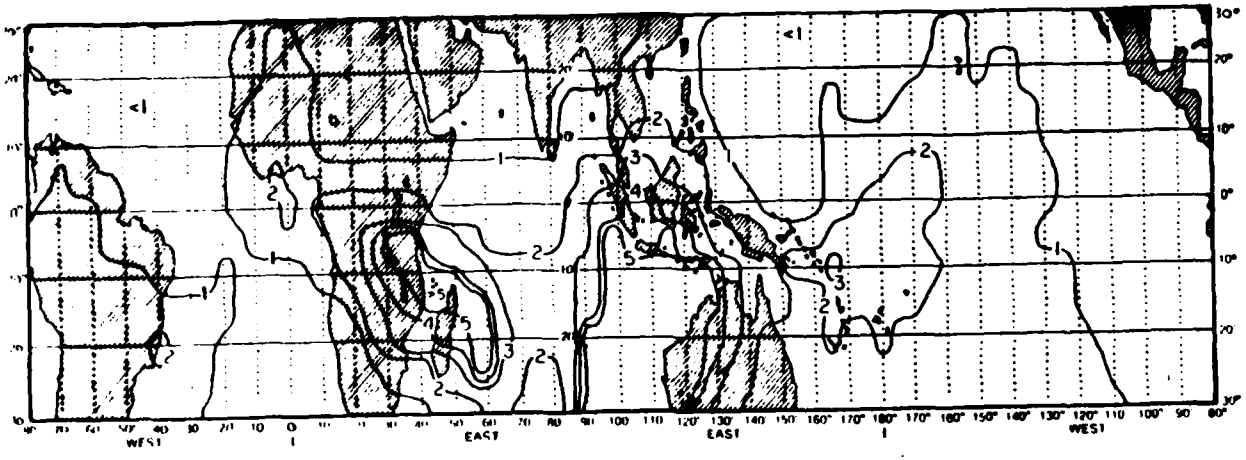

(a)

Figure 9. Root-mean-square wind error, 4 min average, hyperbolic geometry

Observation time: 1200L Noise level: Average (0800-1200L) Dec to Feb Smoothing improvement factor: 3.0
Australia: Non-operational Receiver improvement factor: none Frequency: 13.6 kHz

The contours are given in milliseconds for 4-min average wind errors. The VLF noise power is the average value from CCIR Report No.322 for 0800 to 1200 local time at 13.6 kHz, the Omega frequency used for windfinding.

The Australian Omega station (35^{o}S, 145^{o}E) is non-operational. VLF receiver improvement due to limiting or blanking is negligible. Cubic spline data smoothing decreases the 2-min quadratic error estimate by a factor of 3 (Passi, 1977).

This map is a conservative estimate of local noon wind errors to be expected under stable ionospheric conditions during the Global Weather Experiment when all Omega stations but the Australian station are transmitting at normal (10 kW) radiated power. Bias errors due to diurnal or other ionospheric disturbances are not included. It is assumed that no sferics suppression is provided by the receiving equipment.

The figure is taken from reference 24, which contains a series of such maps for different conditions.

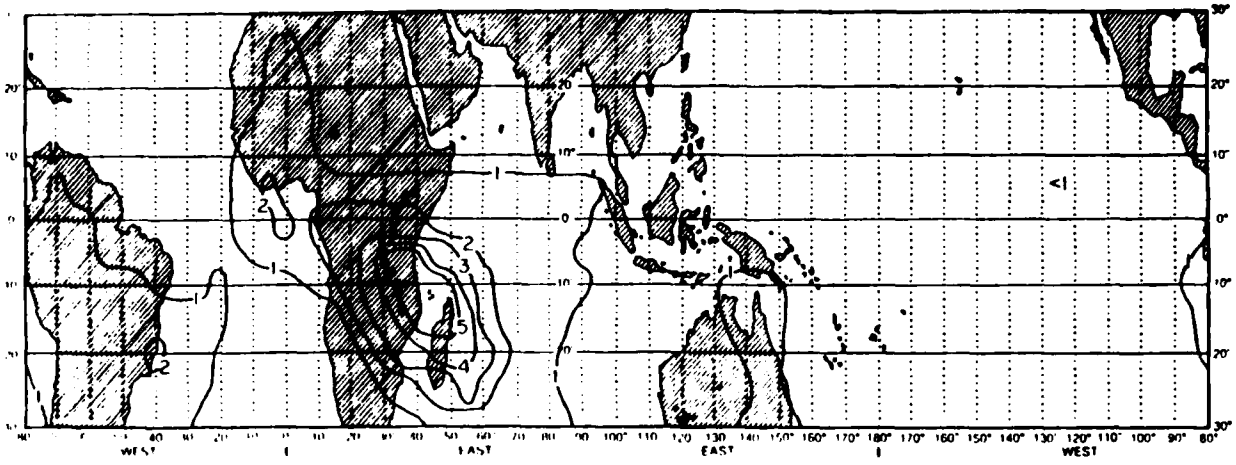

(b)

Figure 9(Contd.).

Observation time: 1200L | Noise level: Average (0800-1200L) Dec to Feb | Smoothing improvement factor: 3.0
Australia: Operational | Receiver improvement factor: None | Frequency: 13.6 kHz

The contours are given in milliseconds for 4-min average wind errors. The VLF noise power is the average value from CCIR Report No. 322 for 0800 to 1200 local time at 13.6 kHz, the Omega frequency used for windfinding.

The Australian Omega station (35^{o}S, 145^{o}E) is operational. VLF receiver improvement due to limiting or blanking is negligible. Cubic spline data smoothing decreases the 2-min quadratic error estimate by a factor of 3 (Passi, 1977).

This map is a conservative estimate of expected errors at local noon when the Omega network of eight stations is fully operational with all stations transmitting at normal radiated power (10 kW). Bias errors due to diurnal or other ionospheric disturbances are not included. It is assumed that no sferics suppression is provided by the receiving equipment.

The high errors over southeast Africa are largely due to high noise levels from thunderstorm activity in this region.

DISTRIBUTION

	Copy No.
DEPARTMENT OF DEFENCE	
Defence Science and Technology Organisation	
Chief Defence Scientist	1
Deputy Chief Defence Scientist	
Controller, External Relations, Projects and Analytical Studies	
Superintendent, Science Programs and Administration	
Defence Science Representative, London	Title page
Counsellor, Defence Science, Washington	Title page
Superintendent, Analytical Studies	2
Superintendent, Major Projects	3
First Assistant Secretary, Defence Industry and Materiel Policy	4
AS, Force Analysis, (Force Development and Analysis)	5
Weapons Systems Research Laboratory	
Director, Weapons Systems Research Laboratory	6
Superintendent, Aeroballistics Division	7
Superintendent, Weapon Systems Division	8
Superintendent, Propulsion Division	9
Head, Ballistics Composite	10
Principal Officer, Ballistic Studies Group	11
Principal Officer, Flight Research Group	12
Principal Officer, Field Experiments Group	13
Principal Officer, Dynamics Group	14
Principal Officer, Aerodynamic Research Group	15
AD Library	16 - 17
Author	18 - 19
Advanced Engineering Laboratory	
Director, Advanced Engineering Laboratory	20

Electronics Research Laboratory

Director, Electronics Research Laboratory	21
Superintendent, Electronics Warfare Division	22
Superintendent, Radar Division	23
Principal Officer, Ionospheric Studies Group	24
Principal Officer, Radio Group	25
Dr K.S.W. Lynn	26
Mr R.S. Edgar	27
Army Projects Officer, DRCS	28

Aeronautical Research Laboratories

Director, Aeronautical Research Laboratories	29

Navy Office

Navy Scientific Adviser	30

Army Office

Scientific Adviser - Army	31 - 35
Director-General of Operations and Plans - Army	36
Director of Operations - Army	37
Director-General, Logistics - Army	38
Director-General of Army Development	39
Director of Operational Requirements, Army	40
Operation Branch (Army) - Artillery (OR7)	41
Director-General of Materiel - Army	42
Director of Armaments and Electronic Materiel - Army (Attention: S01 STASS)	43
School of Artillery (Attention: Commanding Officer/Chief Instructor)	44
(Attention: S1, Locating Wing)	45

Director-General, Army Development (NSO), Russel Offices for ABCA Standardisation Officers

UK ABCA representative, Canberra	46
US ABCA representative, Canberra	47
Canada ABCA representative, Canberra	48
NZ ABCA representative, Canberra	49

Air Office

Air Force Scientific Adviser 50

Staff Officer (Science) HQ1 Division 51

Staff Officer (Science) HQ FF Command 52

Libraries and Information Services

Defence Library, Campbell Park 53

Document Exchange Centre
Defence Information Services Branch for:

Microfilming 54

United Kingdom, Defence Research Information Centre (DRIC) 55 - 56

United States, Defense Technical Information Center 57 - 68

Canada, Director Scientific Information Services 69

New Zealand, Ministry of Defence 70

National Library of Australia 71

Director, Joint Intelligence Organisation (DSTI) 72

Library, Defence Research Centre Salisbury 73 - 74

Library, Aeronautical Research Laboratories 75

Library, Materials Research Laboratories 76

Library, Royal Australian Navy Research Laboratory 77

Library, H Block, Victoria Barracks, Melbourne 78

DEPARTMENT OF DEFENCE SUPPORT

Deputy Secretary (Manufacturing)
Deputy Secretary (Materiel and Resources)
Controller, Defence Aerospace Division
Controller, Munitions Division } 79

Library, DDS Central Office 80

Director, Industry Development, Adelaide Title page

AUSTRALIA

Bureau of Meteorology, Melbourne
(Attention: Mr E. Jesson) 81

UNITED KINGDOM

British Library, Lending Division
Boston Spa Yorks 82

UNITED STATES OF AMERICA

Commandant, US Field Artillery School, Ft Sill, OKLA 73503
(Attention: ATSF-CMS - Mr R. Farmer) 83

NASA Scientific and Technical Information Office 84

Engineering Societies Library 85

Spares 86 - 93

DOCUMENT CONTROL DATA SHEET

Security classification of this page: UNCLASSIFIED

1 DOCUMENT NUMBERS	2 SECURITY CLASSIFICATION
AR Number: AR-003-790	a. Complete Document: Unclassified
Series Number: WSRL-0361-TM	b. Title in Isolation: Unclassified
Other Numbers:	c. Summary in Isolation: Unclassified

3 TITLE

ERROR ANALYSIS OF WIND DETERMINED USING A VLF OMEGA SONDE

4 PERSONAL AUTHOR(S):

K.H. Lloyd

5 DOCUMENT DATE:

June 1984

6 6.1 TOTAL NUMBER OF PAGES 33

6.2 NUMBER OF REFERENCES: 44

7 7.1 CORPORATE AUTHOR(S):

Weapons Systems Research Laboratory

7.2 DOCUMENT SERIES AND NUMBER

Weapons Systems Research Laboratory 0361-TM

8 REFERENCE NUMBERS

a. Task: ARM 81/110

b. Sponsoring Agency:

9 COST CODE:

410028

10 IMPRINT (Publishing organisation)

Defence Research Centre Salisbury

11 COMPUTER PROGRAM(S) (Title(s) and language(s))

12 RELEASE LIMITATIONS (of the document):

Approved for Public Release

Security classification of this page: UNCLASSIFIED

Security classification of this page: UNCLASSIFIED

13 *ANNOUNCEMENT LIMITATIONS (of the information on these pages):*

No limitation

14 DESCRIPTORS:

a. EJC Thesaurus Terms	Wind (meteorology) Determination Omega navigation Error analysis
b. Non-Thesaurus Terms	Sondes AMPARS

15 COSATI CODES:

04020

16 SUMMARY OR ABSTRACT:
(if this is security classified, the announcement of this report will be similarly classified)

The atmospheric wind profile can be determined by tracking the drift of an ascending or descending sonde. Generally the sonde is tracked by radar, but, because of problems associated with radar, Omega navigation is now sometimes used as an alternative. This Memorandum discusses the errors associated with determining the wind profile by using Omega, in particular how the error is related to the rate of descent of the sonde. This study was conducted as part of the AMPARS (Artillery Meteorological Parameters Acquisition Rocket System) feasibility study.

Security classification of this page:

The official documents produced by the Laboratories of the Defence Research Centre Salisbury are issued in one of five categories: Reports, Technical Reports, Technical Memoranda, Manuals and Specifications. The purpose of the latter two categories is self-evident, with the other three categories being used for the following purposes:

Reports	:	documents prepared for managerial purposes.
Technical Reports	:	records of scientific and technical work of a permanent value intended for other scientists and technologists working in the field.
Technical Memoranda	:	intended primarily for disseminating information within the DSTO. They are usually tentative in nature and reflect the personal views of the author.

END

FILMED

4-85

DTIC